JOURNAL OF THERMOPHYSICS AND HEAT TRANSFER
Vol. 24, No. 4, October–December 2010

Spectral Collocation Method for Transient Conduction–Radiation Heat Transfer

Ya-Song Sun* and Ben-Wen Li†
Northeastern University, 110004 Shenyang, People's Republic of China

DOI: 10.2514/1.43400

A spectral collocation method is developed to solve transient coupled conduction and radiation heat transfer problems. For both the radiative transfer equation and the energy equation, the spatial domain is discretized by the spectral collocation method. The angular domain is discretized by the discrete-ordinates method for radiative transfer equation. The formulations and implementation of the spectral collocation with discrete-ordinates method reveal its high efficiency. Because of the exponential convergence of spectral methods in space, a very high accuracy can be obtained, even though a small number of nodes are used for the present problems. Numerical results in one-dimensional planar and two-dimensional rectangular geometries by the spectral collocation with discrete-ordinates method are compared with available results in the literature. These comparisons indicate that the spectral collocation with discrete-ordinates method for transient conduction–radiation heat transfer is accurate and efficient. Effects of various parameters, such as the scattering albedo, the conduction–radiation parameter, and the optical thickness are studied for absorbing, emitting, and isotropically scattering media.

Nomenclature

$\mathbf{A}$	=	matrix defined in Eq. (26a)
$\mathbf{B}$	=	matrix defined in Eq. (26b)
$\mathbf{C}$	=	matrix defined in Eq. (26c)
c_p	=	specific heat of medium, J kg^{-1} K^{-1}
$\mathbf{D}^{(1)}$	=	first-order derivative matrix
$\mathbf{D}^{(2)}$	=	second-order derivative matrix
$\mathbf{F}$	=	matrix defined in Eq. (26d)
h_i, h_j, h_k	=	function of the first-order derivative of Chebyshev polynomials
I	=	radiative intensity, W m^{-2} sr^{-1}
I_b	=	blackbody radiative intensity, W m^{-2} sr^{-1}
i	=	solution node index for x direction
j	=	solution node index for y direction
k	=	solution node index for z direction
k_a	=	absorption coefficient, m^{-1}
k_s	=	scattering coefficient, m^{-1}
L	=	characteristic length, m
M	=	number of discrete-ordinates directions
N	=	total number of spatial solution nodes
N_{cr}	=	conduction–radiation parameter, $\lambda(k_a + k_s)/4\sigma T_{\text{ref}}^3$
N_t	=	number of discretized time steps
N_x	=	total number of collocation points in x direction
N_y	=	total number of collocation points in y direction
N_z	=	total number of collocation points in z direction
$\mathbf{n}_w$	=	unit outward normal vector of boundary
$\mathbf{P}$	=	matrix defined in Eq. (24a)
$\mathbf{Q}$	=	matrix defined in Eq. (24b)
$\mathbf{q}_R$	=	radiative heat flux, W m^{-2}
$\mathbf{R}$	=	matrix defined in Eq. (24c)
$\mathbf{r}$	=	spatial coordinates vector, m
$\mathbf{r}'$	=	dimensionless spatial coordinates vector, $\mathbf{r}/L$
s	=	collocation points
T	=	temperature, K
T_i, T_j, T_k	=	the first kind Chebyshev polynomial
T_{ref}	=	reference temperature, K
t	=	time, s
U	=	Chebyshev collocation points in x direction
u_{ben}	=	benchmark solution
u_{num}	=	numerical solution
$\mathbf{V}$	=	matrix defined in Eq. (24d)
V	=	Chebyshev collocation points in y direction
W	=	Chebyshev collocation points in z direction
w	=	weight of discrete-ordinates approximation, sr
X	=	dimensionless coordinate in x direction, x/L
x	=	coordinate in x direction, m
Y	=	dimensionless coordinate in y direction, y/L
y	=	coordinate in y direction, m
Z	=	dimensionless coordinate in z direction, z/L
z	=	coordinate in z direction, m
ε_E	=	wall emissivity at east boundary
$\varepsilon_{\max}$	=	maximum relative error
ε_W	=	wall emissivity at west boundary
ε_w	=	wall emissivity
ζ	=	dimensionless time, $[\lambda(k_a + k_s)^2 t]/\rho c_p$
$\Delta\zeta$	=	dimensionless time step
η	=	direction cosine in y direction
Θ	=	dimensionless temperature, T/T_{ref}
$\hat{\Theta}$	=	coefficients for spectral approximation in Eq. (21)
λ	=	thermal conductivity, W m^{-1} K^{-1}
μ	=	direction cosine in x direction
ξ	=	direction cosine in z direction
ρ	=	density, kg m^{-3}
σ	=	Stefan–Boltzmann constant, W m^{-2} K^{-4}
τ_L	=	optical thickness, $(k_a + k_s)L$
Φ	=	scattering phase function
Ψ	=	dimensionless radiative intensity, $(\pi I)/(\sigma T_{\text{ref}}^4)$
$\hat{\Psi}$	=	coefficients for spectral approximation in Eq. (21)
$\mathbf{\Omega}$, $\mathbf{\Omega}'$	=	unit vector of radiation direction
ω	=	scattering albedo, $k_s/(k_a + k_s)$

Subscripts

E, W, N, S	=	east, west, north, and south boundaries
i, j, k	=	solution node indexes for x, y, and z directions

Received 23 January 2009; revision received 22 June 2010; accepted for publication 26 June 2010. Copyright © 2010 by the American Institute of Aeronautics and Astronautics, Inc. All rights reserved. Copies of this paper may be made for personal or internal use, on condition that the copier pay the $10.00 per-copy fee to the Copyright Clearance Center, Inc., 222 Rosewood Drive, Danvers, MA 01923; include the code 0887-8722/10 and $10.00 in correspondence with the CCC.

*Ph.D. Student, Key Laboratory of Electromagnetic Processing of Materials (National Education Ministry), 311 Wenhua Road, P.O. Box 314, Heping District.

†Professor, Key Laboratory of Electromagnetic Processing of Materials (National Education Ministry), 311 Wenhua Road, P.O. Box 314, Heping District; heatli@hotmail.com.

l = solution node index
min = minimum value
max = maximum value
w = value at wall

Superscripts

m, m' = angular direction of radiation
n = time step
ζ = dimensionless time, $[\lambda(k_a + k_s)^2 t]/\rho c_p$
$\Delta\zeta$ = dimensionless time step
0 = initial value
$*$ = the last iterative value

I. Introduction

DURING the past five decades, much effort has been expended to solve coupled conduction and radiation heat transfer problems in semitransparent media. The motivation for this effort arises from extensive engineering applications, such as industry furnaces, combustion fabrication devices, glass forming, and the analysis of thermal performance of porous insulating materials. Therefore, research on coupled conduction and radiation heat transfer problems appears to be of practical significance.

Up to now, much research has been performed for coupled conduction and radiation heat transfer in absorbing, emitting, and scattering media. Early in 1962, Viskanta and Grosh [1,2] used an iterative method to analyze coupled conduction and radiation heat transfer between one-dimensional (1-D) parallel plates filled with an absorbing and emitting medium. Razzaque et al. [3] developed a finite element method (FEM) to solve a coupled radiation and conduction heat transfer problem in a two-dimensional (2-D) rectangular enclosure filled with a gray medium. Sakami et al. [4] used the discrete-ordinates method (DOM) to solve a coupled radiation and conduction problem for a 2-D complex geometry. A more recent review on methods addressing coupled radiative and conductive heat transfer can be found in [5]. The integrodifferential radiative transfer equation (RTE) with or without participating media can be solved by many numerical methods [6,7], such as the zonal method, Monte Carlo method, DOM, FEM, finite volume method (FVM). After the determination of the spatial distribution of radiative intensity, or that of the radiative energy sources, the diffusion equation for energy conservation can be solved by the finite difference method (FDM) or FEM.

As for transient coupled conduction and radiation heat transfer in participating planar media, Barker and Sutton [8] and Sutton [9] gave the rigorous formulations using an iterative method in combination with an integral transform technique, and the resulting equations were numerical solved by successive approximation. Tsai and Lin [10] used a finite difference/nodal approximation method to solve this kind of problem; while Yi et al. [11] used a ray-tracing/nodal-analyzing method. Wu and Ou [12] used an integration method to investigate this kind of problem in a rectangular absorbing, emitting, and isotropically scattering media. Liu and Tan [13] studied this kind of problem in a 2-D participating cylinder subjected to a pulse of irradiation. In these processes, the DOM was used to solve the RTE, and an implicit different scheme was employed for handling the energy equation. In [14], the Crank–Nicholson scheme was used to solve the transient energy equation, and the collapsed dimension method (CDM) was applied to solve the radiative part of the energy equation. In [15], the performance evaluation of CDM and the discrete transfer method (DTM) were carried out in terms of computational time and their abilities to provide accurate results. It was found that CDM was much more economical than DTM. In [16–18], the lattice Boltzmann method (LBM) was used to solve the energy equation, and CDM [16], DOM [17], and FVM [18] were adopted to compute the radiative information. In [19], a nonuniform LBM was applied to the solution of the energy equation. Recently, Furmanski and Banaszek [20] developed a new FEM to solve this kind of problem in a 2-D semitransparent media. David et al. [21] studied this kind of problem in nongray semitransparent 2-D media with mixed boundary conditions. Asllanaj et al. [22] studied this kind of problem in a 2-D complex-shaped domain, and a new FVM, based on a cell vertex scheme and associated to a modified exponential scheme, was used to solve the RTE. Luo et al. [23] used a ray-tracing/node-analyzing method to investigate transient coupled heat transfer in a rectangular media.

In the field of numerical simulation, it is well known that the FEM, the FVM, and the FDM can provide linear convergence, while spectral methods can provide exponential convergence [24]. Spectral methods were widely applied in computational fluid dynamics [25,26], electrodynamics [27] and magnetohydrodynamics [28]. Early in 1979, Chawla and Chan [29] used the collocation method, based on B-splines approximating function, to solve combined radiation and conduction problems. Later, Kamiuto [30] developed the Chebyshev collocation method to solve the 1-D RTE. Zenouzi and Yener [31] used the Galerkin method to solve the radiative part of a radiation and natural convection combined problem. Kuo et al. [32] made a numerical comparison between spectral methods and the FVM for solving combined radiation and natural convection problems, and they concluded that spectral methods were more accurate. De Oliveira et al. [33] developed a combination of spectral method and the Laplace transform to solve radiative heat transfer problems in isotropically scattering media. In 2008, the collocation spectral method for the radiative part of stellar modeling was carried out in [34]. Recently, in Modest and Yang's work [35], the spherical harmonics method was further developed to reduce the number of first-order partial differential equations. Researchers [36–41] have successfully developed the Chebyshev collocation spectral method for 1-D radiative heat transfer in anisotropically scattering media [36], 1-D radiative heat transfer in graded refractive index media [37], coupled conduction and radiation in concentric spherical participating media [38], combined radiation and conduction heat transfer in 1-D semitransparent media with graded index [39], transient coupled conduction and radiation in an anisotropically scattering slab with graded index [40], and three-dimensional (3-D) radiative heat transfer [41].

In this paper, we extend the collocation spectral method to solve transient coupled conduction and radiation heat transfer problems in absorbing, emitting, and scattering media. The governing equations are presented in the second section of this paper. The spectral collocation with discrete-ordinates method (SP-DOM) formulations for the RTE and the energy equation and the solution procedure are presented in detail in the third section. Validation using typical cases which are available in the literature is preformed in the fourth section. Finally, the last section gives the conclusions.

II. Governing Equations

For transient coupled conduction and radiation heat transfer problems without heat generation, the energy equation can be written as

$$\rho c_p \frac{\partial T(\mathbf{r}, t)}{\partial t} = \lambda \nabla^2 T(\mathbf{r}, t) - \nabla \cdot \mathbf{q}_R(\mathbf{r}) \tag{1}$$

with the initial and boundary conditions

$$T(\mathbf{r}, 0) = T^0(\mathbf{r}) \tag{2}$$

$$T(\mathbf{r}_w, t) = T|_{\mathbf{r}=\mathbf{r}_w} \tag{3}$$

where $\nabla \cdot \mathbf{q}_R(\mathbf{r})$ is the radiative energy source given by

$$\nabla \cdot \mathbf{q}_R(\mathbf{r}) = k_a[4\pi I_b(\mathbf{r}) - \int_{4\pi} I(\mathbf{r}, \mathbf{\Omega})\, \mathrm{d}\mathbf{\Omega}] \tag{4}$$

In the Cartesian coordinate system, assuming that the medium is gray and neglecting the transient radiative term, since the radiative propagation time is much faster than the thermal response of the medium, the governing equation for radiative transfer in terms of

radiation intensity in absorbing, emitting, and scattering media can be expressed as

$$(\boldsymbol{\Omega}\cdot\nabla)I(\mathbf{r},\boldsymbol{\Omega}) = -(k_a+k_s)I(\mathbf{r},\boldsymbol{\Omega}) + k_a I_b(\mathbf{r}) + \frac{k_s}{4\pi}\int_{4\pi} I(\mathbf{r},\boldsymbol{\Omega}')\Phi(\boldsymbol{\Omega}',\boldsymbol{\Omega})\,\mathrm{d}\boldsymbol{\Omega}' \tag{5}$$

For an opaque and diffuse boundary, the boundary condition is given as

$$I(\mathbf{r}_w,\boldsymbol{\Omega}) = \varepsilon_w I_b(\mathbf{r}_w) + \frac{1-\varepsilon_w}{\pi}\int_{\mathbf{n}_w\cdot\boldsymbol{\Omega}'>0} I(\mathbf{r}_w,\boldsymbol{\Omega}')|\mathbf{n}_w\cdot\boldsymbol{\Omega}'|\mathrm{d}\boldsymbol{\Omega}', \qquad \mathbf{n}_w\cdot\boldsymbol{\Omega}<0 \tag{6}$$

For convenience of analysis, the energy equation and the RTE together with their initial and boundary conditions are nondimensionalized as

$$\frac{\partial\Theta(\mathbf{r}',\zeta)}{\partial\zeta} = \frac{1}{\tau_L^2}\nabla^2\Theta(\mathbf{r}',\zeta) - \frac{(1-\omega)}{N_{\mathrm{cr}}}\left[\Theta^4(\mathbf{r}',\zeta) - \frac{1}{4\pi}\int_{4\pi}\Psi(\mathbf{r}',\boldsymbol{\Omega},\zeta)\,\mathrm{d}\boldsymbol{\Omega}\right] \tag{7}$$

$$\Theta(\mathbf{r}',0) = \Theta^0(\mathbf{r}') \tag{8}$$

$$\Theta(\mathbf{r}'_w,t) = \Theta|_{\mathbf{r}'=\mathbf{r}'_w} \tag{9}$$

$$\frac{1}{\tau_L}(\boldsymbol{\Omega}\cdot\nabla)\Psi(\mathbf{r}',\boldsymbol{\Omega}) + \Psi(\mathbf{r}',\boldsymbol{\Omega}) = (1-\omega)\Theta^4(\mathbf{r}') + \frac{\omega}{4\pi}\int_{4\pi}\Psi(\mathbf{r}',\boldsymbol{\Omega}')\Phi(\boldsymbol{\Omega}',\boldsymbol{\Omega})\,\mathrm{d}\boldsymbol{\Omega}' \tag{10}$$

$$\Psi(\mathbf{r}'_w,\boldsymbol{\Omega}) = \varepsilon_w\Theta^4(\mathbf{r}'_w) + \frac{1-\varepsilon_w}{\pi}\int_{\mathbf{n}_w\cdot\boldsymbol{\Omega}'>0}\Psi(\mathbf{r}'_w,\boldsymbol{\Omega}')|\mathbf{n}_w\cdot\boldsymbol{\Omega}'|\mathrm{d}\boldsymbol{\Omega}', \qquad \mathbf{n}_w\cdot\boldsymbol{\Omega}<0 \tag{11}$$

III. Discretization of the Energy Equation and the RTE, and the Solution Procedure

A. Temporal Discretization of the Energy Equation

Using the fully implicit difference scheme, the temporal discretization of the energy equation (7) reads

$$\frac{\Theta^{\zeta+\Delta\zeta}-\Theta^{\zeta}}{\Delta\zeta} = \frac{1}{\tau_L^2}\nabla^2\Theta^{\zeta+\Delta\zeta} - \frac{(1-\omega)}{N_{\mathrm{cr}}}\left[(\Theta^{\zeta+\Delta\zeta})^4 - \frac{1}{4\pi}\sum_{m'=1}^{M}\Psi^{m,\zeta+\Delta\zeta}w^m\right] \tag{12}$$

The fully implicit scheme is unconditionally stable. Equation (12) can be expressed as

$$\frac{\Delta\zeta}{\tau_L^2}\nabla^2\Theta^{n+1} - \frac{\Delta\zeta}{N_{\mathrm{cr}}}(1-\omega)(\Theta^{n+1})^4 - \Theta^{n+1} = -\frac{\Delta\zeta}{N_{\mathrm{cr}}}(1-\omega)\frac{1}{4\pi}\sum_{m=1}^{M}\Psi^{m,n+1}w^m - \Theta^n \tag{13}$$

Equation (13) is a strongly nonlinear partial differential equation. To reduce the nonlinearity, we rewrite it in a new equivalent form as in [38] for the convenience of spatial discretization later:

$$\frac{\Delta\zeta}{\tau_L^2}\nabla^2\Theta^{n+1} - \frac{2\Delta\zeta}{N_{\mathrm{cr}}}(1-\omega)(\Theta^{n+1})^4 - \Theta^{n+1} = -\frac{\Delta\zeta}{N_{\mathrm{cr}}}(1-\omega)\left[(\Theta^{n+1})^4 + \frac{1}{4\pi}\sum_{m'=1}^{M}\Psi^{m,n+1}w^m\right] - \Theta^n \tag{14}$$

B. Discrete-Ordinates Equation of the RTE

The discretized form of the RTE is obtained by evaluating Eq. (10) in each discrete direction and replacing the integral by a numerical quadrature to give

$$\frac{1}{\tau_L}\left[\mu^m\frac{\partial\Psi(\mathbf{r}',\boldsymbol{\Omega}^m)}{\partial X} + \eta^m\frac{\partial\Psi(\mathbf{r}',\boldsymbol{\Omega}^m)}{\partial Y} + \xi^m\frac{\partial\Psi(\mathbf{r}',\boldsymbol{\Omega}^m)}{\partial Z}\right] + \Psi(\mathbf{r}',\boldsymbol{\Omega}^m) = (1-\omega)\Theta^4(\mathbf{r}') + \frac{\omega}{4\pi}\sum_{m'=1}^{M}\Psi(\mathbf{r}',\boldsymbol{\Omega}^{m'})\Phi^{m',m}w^{m'}, \qquad m=1,2,\cdots,M \tag{15}$$

The discrete-ordinates representation of the boundary condition, Eq. (11), is given by

$$\Psi(\mathbf{r}'_w,\boldsymbol{\Omega}^m) = \varepsilon_w\Theta^4(\mathbf{r}'_w) + \frac{1-\varepsilon_w}{\pi}\sum_{m'=1,\mathbf{n}_w\cdot\boldsymbol{\Omega}^{m'}>0}^{M}\Psi(\mathbf{r}'_w,\boldsymbol{\Omega}^{m'})|\mathbf{n}_w\cdot\boldsymbol{\Omega}^{m'}|w^{m'}, \qquad \mathbf{n}_w\cdot\boldsymbol{\Omega}^m<0, \qquad m=1,2,\cdots,M \tag{16}$$

C. Chebyshev Collocation Spectral Formulation

The Chebyshev–Gauss–Lobatto collocation points are used for spatial discretization:

$$\begin{cases} U_i = -\cos\frac{\pi i}{N_x}, & i=0,1,\ldots,N_x \\ V_j = -\cos\frac{\pi j}{N_y}, & j=0,1,\ldots,N_y \\ W_k = -\cos\frac{\pi k}{N_z}, & k=0,1,\ldots,N_z \end{cases} \tag{17}$$

The mappings of arbitrary intervals $[X_{\min},X_{\max}]\times[Y_{\min},Y_{\max}]\times[Z_{\min},Z_{\max}]$ to standard intervals $[-1,1]\times[-1,1]\times[-1,1]$ are needed to fit the requirements of the Chebyshev collocation spectral method:

$$\begin{cases} U = \frac{2X-(X_{\max}+X_{\min})}{X_{\max}-X_{\min}}, & X = \frac{U(X_{\max}-X_{\min})+(X_{\max}+X_{\min})}{2} \\ V = \frac{2Y-(Y_{\max}+Y_{\min})}{Y_{\max}-Y_{\min}}, & Y = \frac{V(Y_{\max}-Y_{\min})+(Y_{\max}+Y_{\min})}{2} \\ W = \frac{2Z-(Z_{\max}+Z_{\min})}{Z_{\max}-Z_{\min}}, & Z = \frac{W(Z_{\max}-Z_{\min})+(Z_{\max}+Z_{\min})}{2} \end{cases} \tag{18}$$

After interval mapping, Eqs. (14) and (15) become

$$\frac{\Delta\zeta}{\tau_L^2}\left[\left(\frac{2}{X_{\max}-X_{\min}}\right)^2\frac{\partial^2\Theta^{n+1}}{\partial U^2} + \left(\frac{2}{Y_{\max}-Y_{\min}}\right)^2\frac{\partial^2\Theta^{n+1}}{\partial V^2} + \left(\frac{2}{Z_{\max}-Z_{\min}}\right)^2\frac{\partial^2\Theta^{n+1}}{\partial W^2}\right] - \frac{2\Delta\zeta}{N_{\mathrm{cr}}}(1-\omega)(\Theta^{n+1})^4 - \Theta^{n+1} = -\frac{\Delta\zeta}{N_{\mathrm{cr}}}(1-\omega)\left[(\Theta^{n+1})^4 + \frac{1}{4\pi}\sum_{m=1}^{M}\Psi^{m,n+1}w^m\right] - \Theta^n \tag{19}$$

$$\frac{\mu^m}{\tau_L}\left(\frac{2}{X_{\max}-X_{\min}}\right)\frac{\partial\Psi^m}{\partial U} + \frac{\eta^m}{\tau_L}\left(\frac{2}{Y_{\max}-Y_{\min}}\right)\frac{\partial\Psi^m}{\partial V} + \frac{\xi^m}{\tau_L}\left(\frac{2}{Z_{\max}-Z_{\min}}\right)\frac{\partial\Psi^m}{\partial W} + \Psi^m = (1-\omega)\Theta^4 + \frac{\omega}{4\pi}\sum_{m'=1}^{M}\Psi^{m'}\Phi^{m',m}w^{m'}, \qquad m=1,2,\cdots,M \tag{20}$$

The dimensionless temperature and the dimensionless radiative intensity can be approximated by

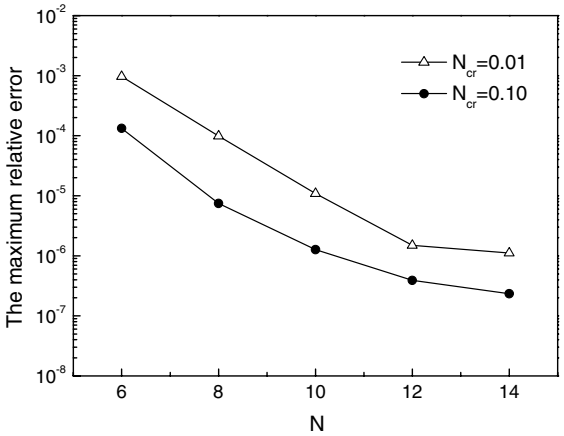

Fig. 1 Exponential convergence rate of the spectral collocation method according to total number of spatial solution nodes.

$$\begin{cases} \Theta(U,V,W) = \sum_{i=0}^{N_x}\sum_{j=0}^{N_y}\sum_{k=0}^{N_z}\hat{\Theta}_{i,j,k}T_i(U)T_j(V)T_k(W) \\ \Psi^m(U,V,W) = \sum_{i=0}^{N_x}\sum_{j=0}^{N_y}\sum_{k=0}^{N_z}\hat{\Psi}_{i,j,k}T_i(U)T_j(V)T_k(W) \end{cases} \tag{21}$$

The polynomials of degree N_x, N_y, and N_z defined by Eq. (21) can be the Lagrange interpolation polynomial based on the sets $\{U_i\}$, $\{V_j\}$, and $\{W_k\}$, such as

$$\begin{cases} \Theta(U,V,W) = \sum_{i=0}^{N_x}\sum_{j=0}^{N_y}\sum_{k=0}^{N_z}h_i(U)h_j(V)h_k(W)\Theta(U_i,V_j,W_k) \\ \Psi^m(U,V,W) = \sum_{i=0}^{N_x}\sum_{j=0}^{N_y}\sum_{k=0}^{N_z}h_i(U)h_j(V)h_k(W)\Psi^m(U_i,V_j,W_k) \end{cases} \tag{22}$$

Table 1 Effects of various combinations of nodes and angular directions in SP-DOM on dimensionless temperature at three locations for $\tau_L = 1.0$, $\omega = 0.5$, $N_{\mathrm{cr}} = 0.1$, and $T_E = 0.5T_{\mathrm{ref}}$

N	M	$X = 0.25$	$X = 0.50$	$X = 0.75$
6	4	0.8923	0.7923	0.6682
10	6	0.8922	0.7924	0.6685
14	8	0.8922	0.7925	0.6688
20	10	0.8922	0.7925	0.6689
40	12	0.8922	0.7926	0.6689

To avoid solving for spectral coefficients and performing fast cosine transformation, we use Eq. (22) rather than Eq. (21) in Eqs. (19) and (20).

D. Discretization and Numerical Implementation

Substituting Eq. (22) into Eq. (19), one can obtain the spectral discretized linear equation:

$$\sum_{l=0}^{N_x}P_{il}\Theta_{ljk} + \sum_{l=0}^{N_y}Q_{jl}\Theta_{ilk} + \sum_{l=0}^{N_z}R_{kl}\Theta_{ijl} - \frac{2\Delta\zeta}{N_{\mathrm{cr}}}(1-\omega)(\Theta^*_{ijk})^3\Theta_{ijk} = V_{ijk} \tag{23}$$

where the elemental expressions for matrices **P**, **Q**, **R**, and **V** are

$$P_{il} = \begin{cases} \frac{\Delta\zeta}{\tau_L^2}\left(\frac{2}{X_{\max}-X_{\min}}\right)^2 D_{il}^{(2)} - 1, & i = l \\ \frac{\Delta\zeta}{\tau_L^2}\left(\frac{2}{X_{\max}-X_{\min}}\right)^2 D_{il}^{(2)}, & i \neq l \end{cases} \tag{24a}$$

$$Q_{jl} = \frac{\Delta\zeta}{\tau_L^2}\left(\frac{2}{Y_{\max}-Y_{\min}}\right)^2 D_{jl}^{(2)} \tag{24b}$$

$$R_{kl} = \frac{\Delta\zeta}{\tau_L^2}\left(\frac{2}{Z_{\max}-Z_{\min}}\right)^2 D_{kl}^{(2)} \tag{24c}$$

$$V_{ijk} = -\frac{\Delta\zeta}{N_{\mathrm{cr}}}(1-\omega)\left[(\Theta^{*,n+1}_{ijk})^4 + \frac{1}{4\pi}\sum_{m=1}^{M}\Psi^{m,n+1}_{ijk}w^m\right] - \Theta^n_{ijk} \tag{24d}$$

Similarly, the spectral discretization of the RTE can be written in matrix form:

$$\sum_{l=0}^{N_x}A^m_{il}\Psi^m_{ljk} + \sum_{l=0}^{N_y}B^m_{jl}\Psi^m_{ilk} + \sum_{l=0}^{N_z}C^m_{kl}\Psi^m_{ijl} = F^m_{ijk}, \qquad m = 1,2,\ldots,M \tag{25}$$

where the elemental expressions for matrices $\mathbf{A}^m$, $\mathbf{B}^m$, $\mathbf{C}^m$, and $\mathbf{F}^m$ are

Table 2 The transient dimensionless temperature Θ at dimensionless time $\zeta = 0.05$ for $\tau_L = 1.0$, $\omega = 0.5$, $N_{\mathrm{cr}} = 1.0$, and $T_E = 0.0$ and two sets of wall reflectivities[a]

Investigators	Transient temperature Θ $X = 0.25$	$X = 0.50$	$X = 0.75$
	$\varepsilon_W = 1.0$, $\varepsilon_E = 1.0$		
Talukdar and Mishra [14]	0.4892	0.1768	0.0585
Barker and Sutton [8]	0.4893 (0.02%)	0.1775 (0.40%)	0.0588 (0.51%)
Sutton [9]	0.4888 (0.08%)	0.1778 (0.57%)	0.0591 (1.03%)
Tsai and Lin [10]	0.4889 (0.06%)	0.1773 (0.28%)	0.0588 (0.51%)
Mishra and Roy [18]	0.4897 (0.10%)	0.1771 (0.17%)	0.0581 (0.68%)
Mondal and Mishra [19]	0.4898 (0.12%)	0.1771 (0.17%)	0.0581 (0.68%)
SP-DOM (present)	0.4888 (0.08%)	0.1771 (0.17%)	0.0587 (0.34%)
	$\varepsilon_W = 1.0$, $\varepsilon_E = 0.0$		
Talukdar and Mishra [14]	0.5033	0.1995	0.0824
Barker and Sutton [8]	0.5035 (0.04%)	0.2003 (0.40%)	0.0831 (0.85%)
Sutton [9]	0.5030 (0.06%)	0.2005 (0.50%)	0.0833 (1.09%)
Tsai and Lin [10]	0.5031 (0.04%)	0.2001 (0.30%)	0.0830 (0.73%)
Mishra and Roy [18]	0.4996 (0.74%)	0.1991 (0.20%)	0.0820 (0.49%)
Mondal and Mishra [19]	0.5018 (0.30%)	0.1965 (1.50%)	0.0817 (0.85%)
SP-DOM (present)	0.5031 (0.04%)	0.1998 (0.15%)	0.0826 (0.24%)

[a]Numbers in parentheses are relative errors compared with [14].

$$A_{il}^m = \begin{cases} \frac{\mu^m}{\tau_L}\left(\frac{2}{X_{\max}-X_{\min}}\right)D_{il}^{(1)} + 1, & i = l \\ \frac{\mu^m}{\tau_L}\left(\frac{2}{X_{\max}-X_{\min}}\right)D_{il}^{(1)}, & i \neq l \end{cases} \tag{26a}$$

$$B_{jl}^m = \frac{\eta^m}{\tau_L}\left(\frac{2}{Y_{\max}-Y_{\min}}\right)D_{jl}^{(1)} \tag{26b}$$

$$C_{kl}^m = \frac{\xi^m}{\tau_L}\left(\frac{2}{Z_{\max}-Z_{\min}}\right)D_{kl}^{(1)} \tag{26c}$$

$$F_{ijk}^m = (1-\omega)\Theta_{ijk}^4 + \frac{\omega}{4\pi}\sum_{m'=1}^{M}\Psi_{ijk}^{m'}\Phi^{m',m}w^{m'} \tag{26d}$$

The implementation of the Chebyshev collocation spectral method for solving transient coupled conduction and radiation heat transfer problems can be executed through the following routine:

Step 1: Choose the resolution (number of collocation points) N_x, N_y, and N_z, compute the coordinate values of nodes using Eqs. (17)

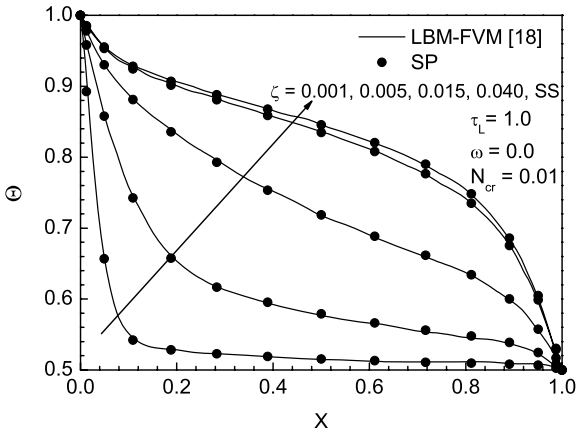

a)

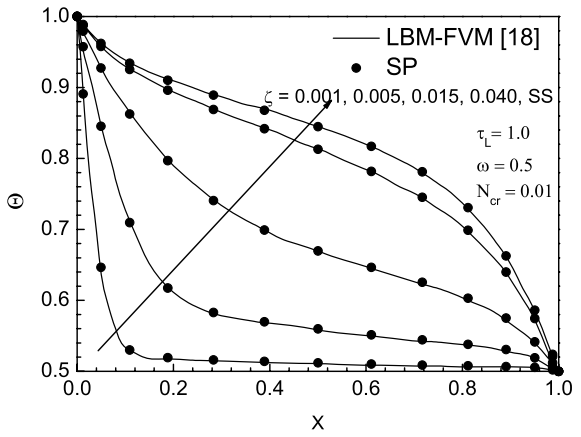

b)

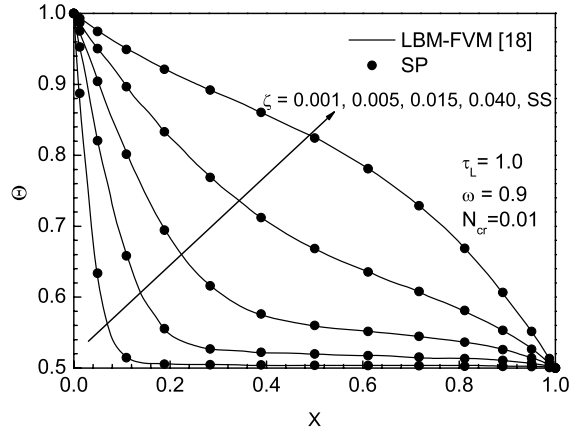

c)

Fig. 2 Dimensionless temperature Θ in a planar medium at different instants ζ for scattering albedo: a) $\omega = 0.0$, b) $\omega = 0.5$, and c) $\omega = 0.9$.

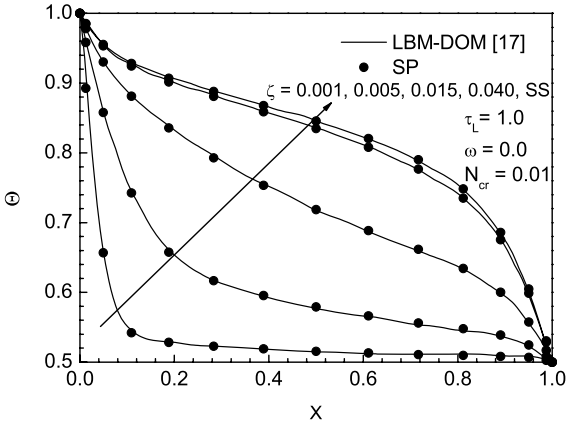

a)

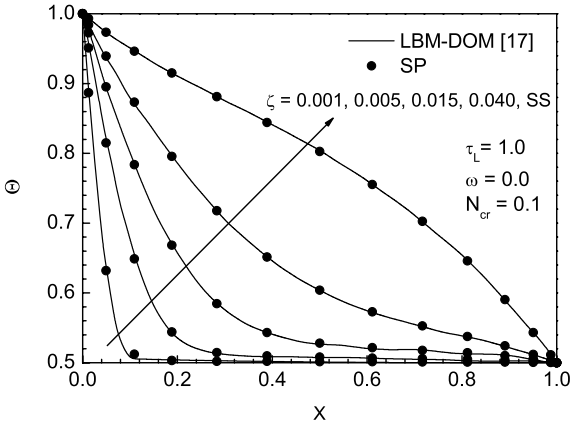

b)

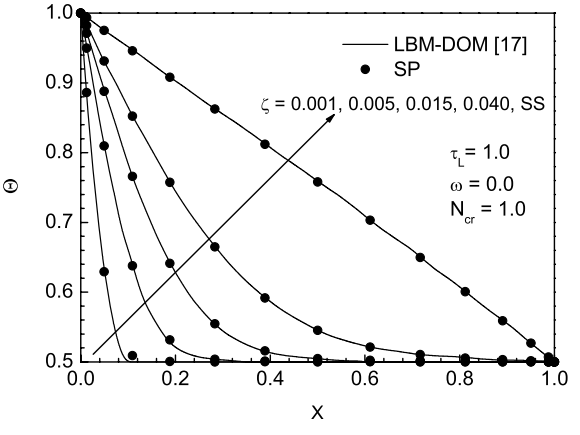

c)

Fig. 3 Dimensionless temperature Θ in a planar medium at different instants ζ for conduction–radiation parameter: a) $N_{cr} = 0.01$, b) $N_{cr} = 0.1$, and c) $N_{cr} = 1.0$.

and (18), and give the radiative intensity and the temperature initial assumptions (zero, for example), except for boundary conditions.

Step 2: Compute matrices $\mathbf{A}$, $\mathbf{B}$, $\mathbf{C}$, $\mathbf{D}^{(1)}$, $\mathbf{D}^{(2)}$, $\mathbf{P}$, $\mathbf{Q}$, and $\mathbf{R}$ once for all [Eqs. (24a–24c) and (26a–26c)].

Step 3: Loop at each time step, $n = 1, 2, \ldots, N_t$.

Step 4: Calculate the matrix $\mathbf{V}$ [Eq. (24d)], impose the boundary condition [Eq. (9)], and directly solve Eq. (23).

Step 5: Calculate the matrix $\mathbf{F}^m$ [Eq. (26d)], impose the boundary condition [Eq. (16)], and directly solve Eq. (25) in each angular direction.

Step 6: Terminate the iteration if the relative maximum absolute difference between two consecutive iterates for the dimensionless radiative intensities for all nodes and directions or for dimensionless temperatures for all nodes are less than the tolerance (10^{-6}, for example); otherwise, go back to step 4.

Step 7: If the maximum time has not been reached, go to step 3, else do postprocessing.

From the above steps, the most important steps, specifically for the matrix equations solution, steps 4 and 5, can be executed directly and efficiently, while other steps are only concerned with assembling the matrices.

IV. Results and Discussion

In our present work, we consider transient conduction and radiation heat transfer problems in 1-D planar and 2-D square geometries. For these problems, the angular domain is discretized by the DOM, and the spatial domain is discretized by the spectral collocation method.

A. Coupled Conduction and Radiation Heat Transfer in a One-Dimensional Planar Medium

In this case, initially the medium is at temperature T_E. From time $t \geq 0$, the west boundary is maintained at $T_W = T_{\text{ref}}$. The conducting–radiating medium is considered to be absorbing, emitting, and isotropically scattering. The medium boundaries are assumed to be diffuse gray. Thermophysical properties are constant. Benchmark results for this problem are available in [8–10,14,18,19].

In the SP-DOM, the dimensionless time step $\Delta\zeta = 1.0 \times 10^{-4}$ is used, and steady-state conditions are assumed to have been achieved when the maximum absolute difference of dimensionless temperature Θ at any location between two consecutive time steps does not exceed 1.0×10^{-6}. The exponential convergence characteristic of spectral methods is studied for two values of conduction–radiation parameter: namely, $N_{\text{cr}} = 0.01$ and 0.1. Figure 1 shows the exponential convergence characteristic of spectral methods against the resolution for the case of optical thickness $\tau_L = 1.0$, scattering albedo $\omega = 0.5$, and initial temperature $T_E = 0.5T_{\text{ref}}$, where the solution obtained using $N = 50$ is considered as the benchmark solution. It can be seen that the convergence rate is very fast for different values of conduction–radiation parameter and approximately follows an exponential law trend.

For the sake of quantitative comparison to the benchmark solution, the maximum relative error is defined as

$$\varepsilon_{\max} = \max\left(\frac{|u_{\text{num}} - u_{\text{ben}}|}{|u_{\text{ben}}|}\right) \times 100\% \tag{27}$$

Then we investigated the effect of various combinations of nodes and angular directions on dimensionless temperature Θ by comparing the steady-state results at three locations. Results obtained for optical thickness $\tau_L = 1.0$, scattering albedo $\omega = 0.5$, conduction–radiation parameter $N_{\text{cr}} = 0.1$, and initial temperature $T_E = 0.5T_{\text{ref}}$, are listed in Table 1. It can be seen that with the combination of $N = 14$ and $M = 8$, the maximum variation in dimensionless temperature is less than 4.3561×10^{-5}. A similar trend is observed for other sets of parameters and therefore need not be reproduced here. For subsequent computations, the number of nodes $N = 14$ is used for spatial discretization, and the total solid angle is subdivided into $M = 8$ directions.

In Table 2, for the two sets of boundary emissivities, the SP-DOM results for dimensionless temperature Θ at three locations in the medium ($X = 0.25$, 0.5, and 0.75) are compared at dimensionless time $\zeta = 0.05$ with those reported in [8–10,14,18,19]. For this comparison, the entire system is initially considered to be cold $T_E = 0.0$ and the west boundary is maintained at $T_W = T_{\text{ref}}$. The values of the parameters are optical thickness $\tau_L = 1.0$, scattering albedo $\omega = 0.5$, and conduction–radiation parameter $N_{\text{cr}} = 0.1$. Table 2 clearly shows that the SP-DOM results agree with those of Talukdar and Mishra [14], Barker and Sutton [8], Sutton [9], Tsai and Lin [10], Mishra and Roy [18], and Mondal and Mishra [19]. Here, the number of nodes $N = 14$ is used for the SP-DOM; however, 100 control volumes/lattices are used in [18] for the LBM-FVM and the FVM-FVM. When the same accuracy is needed, very few nodes are needed by SP-DOM, hence saving computational resources. The reason is that for LBM and FVM, the computation at any lattice/volume involves only very few neighboring lattice/volume values, while the spectral methods are global methods, where the computation at any given point depends on information from the entire domain [24–26,42].

For $\tau_L = 1.0$, $N_{\text{cr}} = 0.01$, and $T_E = 0.5T_{\text{ref}}$, the SP-DOM approximation of the dimensionless temperature Θ at different

Table 3 Steady-state dimensionless temperature Θ at three locations on centerline ($X = 0.5$) in a black square enclosure; $\omega = 0.0$[a]

Centerline Θat Y	Mishra et al. [15]	Wu and Ou [12]	Mondal and Mishra [19]	Yuen and Takara [44]	SP-DOM (present)
			$\beta = 0.1$, $N_{\text{cr}} = 0.1$		
0.3	0.734	0.733 (0.14%)	0.734 (0.00%)	0.733 (0.14%)	0.735 (0.14%)
0.5	0.626	0.626 (0.00%)	0.626 (0.00%)	0.630 (0.64%)	0.626 (0.00%)
0.7	0.561	0.561 (0.00%)	0.561 (0.00%)	0.563 (0.36%)	0.560 (0.18%)
			$\beta = 1.0$, $N_{\text{cr}} = 1.0$		
0.3	0.737	0.733 (0.54%)	0.737 (0.00%)	0.737 (0.00%)	0.737 (0.00%)
0.5	0.630	0.630 (0.00%)	0.630 (0.00%)	0.630 (0.00%)	0.630 (0.00%)
0.7	0.564	0.560 (0.71%)	0.564 (0.00%)	0.560 (0.71%)	0.564 (0.00%)
			$\beta = 1.0$, $N_{\text{cr}} = 0.1$		
0.3	0.759	0.760 (0.13%)	0.759 (0.00%)	0.763 (0.53%)	0.759 (0.00%)
0.5	0.663	0.663 (0.00%)	0.664 (0.15%)	0.661 (0.30%)	0.662 (0.15%)
0.7	0.594	0.590 (0.67%)	0.596 (0.34%)	0.589 (0.84%)	0.594 (0.00%)
			$\beta = 1.0$, $N_{\text{cr}} = 0.01$		
0.3	0.789	0.791 (0.25%)	0.784 (0.63%)	0.807 (2.28%)	0.786 (0.38%)
0.5	0.725	0.725 (0.00%)	0.726 (0.14%)	0.726 (0.14%)	0.724 (0.14%)
0.7	0.666	0.663 (0.45%)	0.678 (1.80%)	0.653 (1.95%)	0.669 (0.45%)
			$\beta = 5.0$, $N_{\text{cr}} = 0.1$		
0.3	0.802	0.834 (3.99%)	0.800 (0.25%)	0.802 (0.00%)	0.795 (0.87%)
0.5	0.706	0.689 (2.41%)	0.706 (0.00%)	0.707 (0.14%)	0.706 (0.00%)
0.7	0.626	0.585 (6.55%)	0.625 (0.16%)	0.626 (0.00%)	0.628 (0.32%)

[a]Numbers in parentheses are relative errors compared with [15].

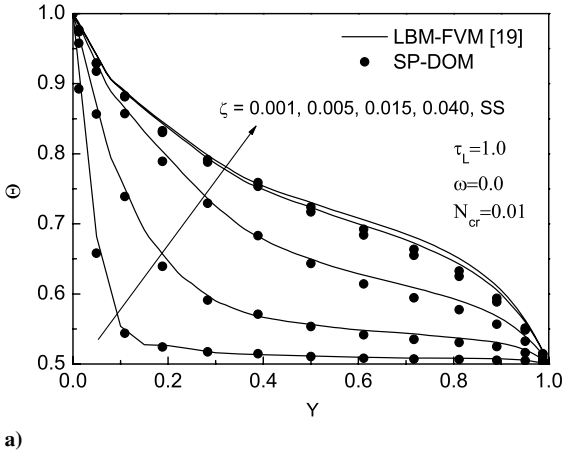

a)

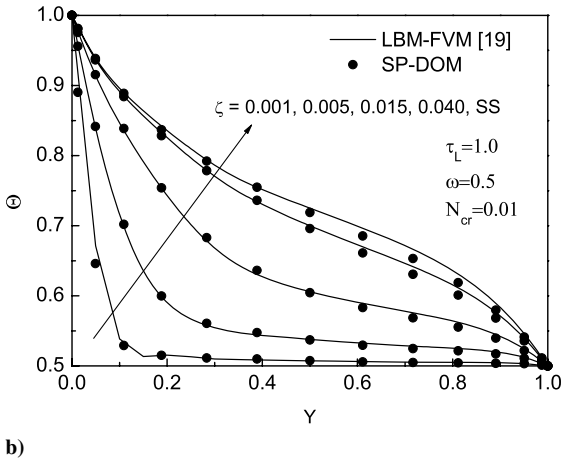

b)

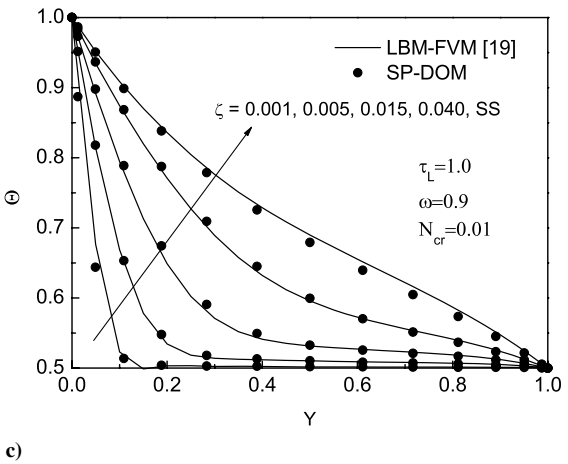

c)

Fig. 4 Dimensionless temperature Θ on centerline ($X = 0.5$) in a square enclosure at different instants ζ for scattering albedo: a) $\omega = 0.0$, b) $\omega = 0.5$, and c) $\omega = 0.9$.

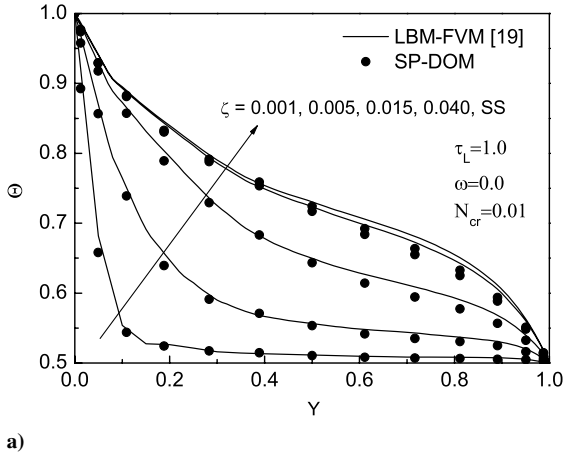

a)

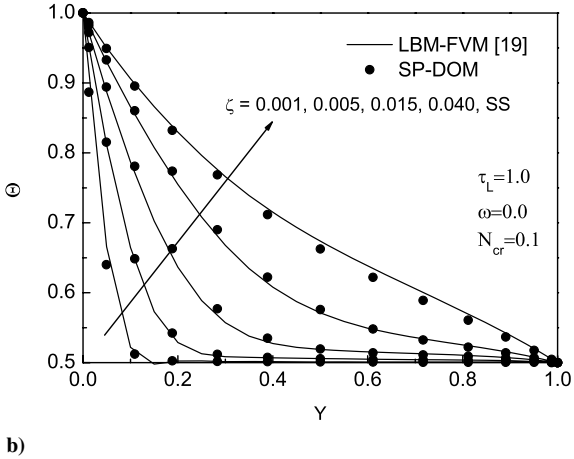

b)

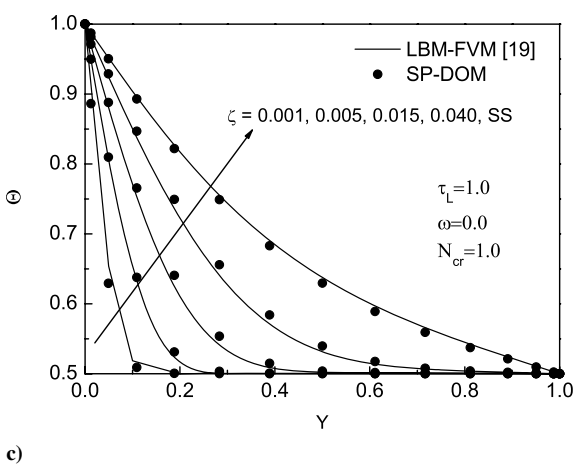

c)

Fig. 5 Dimensionless temperature Θ on centerline ($X = 0.5$) in a square enclosure at different instants ζ for conduction–radiation parameter: a) $N_{cr} = 0.01$, b) $N_{cr} = 0.1$, and c) $N_{cr} = 1.0$.

instants of dimensionless time ζ for three scattering albedo of $\omega = 0.0, 0.5$, and 0.9 are shown in Fig. 2, and compared to the results obtained by Mishra and Roy [18]. The SP-DOM results are very close to those of the LBM-FVM [18]. The maximum relative error of the SP-DOM results is less than 2.4738%.

In Fig. 3, the dimensionless temperatures Θ of the SP-DOM and the LBM-DOM [17] are compared for different N_{cr} With $\tau_L = 1.0$, $\omega = 0.0$ and initial temperature $T_E = 0.5T_{ref}$, these comparisons are shown in Figs. 3a–3c for $N_{cr} = 0.01$, 0.1, and 1.0, respectively. It can be seen that for both radiation-dominated ($N_{cr} = 0.01$) and conduction-dominated ($N_{cr} = 1.0$) situations, the results of the SP-DOM and the LBM-DOM are in good agreement with each other. The maximum percentage errors between the SP-DOM and the LBM-DOM are 1.2588, 1.3248, and 1.8331% for $N_{cr} = 0.01$, 0.1, and 1.0, respectively. For $N_{cr} = 1.0$, in the early stages where $\zeta = 0.001$ and 0.005, the SP-DOM results at some distance from the hot (west) boundary are higher than the LBM-DOM results. The reason is that the convergence rates are different for spectral methods and the LBM, and transient results may differ to some degree.

B. Coupled Conduction and Radiation Heat Transfer in a Two-Dimensional Square-Enclosure Medium

For a 2-D square transient coupled conduction and radiation heat transfer problem, the initial temperatures of the east wall, the west wall, the north wall, and the medium are $T_E = T_W = T_N = T_0 = 0.5T_{\text{ref}}$. From $t \geq 0$, the temperature of the south boundary is $T_S = T_{\text{ref}}$. The conducting–radiating medium is considered to be absorbing, emitting, and isotropically scattering. The medium boundaries are assumed to be diffuse gray. The thermophysical properties are held constant.

In this 2-D case, the dimensionless time step $\Delta\zeta = 1.0 \times 10^{-4}$ is used as in the 1-D case, and steady-state conditions are assumed to have been achieved when the maximum temperature at any location between two consecutive time steps does not exceed 1.0×10^{-6}. For this case, the number of nodes $N_x \times N_y = 14 \times 14$ is used for spatial discretization, and the total solid angle is subdivided into 80 directions (SSD_{3b} approximation [43]).

The dimensionless temperatures Θ at three Y locations on the centerline ($X = 0.5$) in the case of scattering albedo $\omega = 0.0$ are listed in Table 3. The results from the SP-DOM are compared with those of Wu and Ou [12], Mishra et al. [15], Mondal and Mishra [19], and Yuen and Takara [44]. From Table 3, it is clearly seen that the SP-DOM can provide more accurate results than those of Wu and Ou [12], Mondal and Mishra [19], and Yuen and Takara [44]. Here, CDM results [15] are chosen as benchmark results. CDM has been found to be successful for both pure radiative [15,45] and combined problems [14,15,46]. It gives very accurate results for optically very thin to very thick cases. In addition, in [15], CDM is found to be more economical than the DTM.

For $\tau_L = 1.0$ and $N_{\text{cr}} = 0.01$, Fig. 4 shows the dimensionless temperatures Θ at different instants ζ on the centerline ($X = 0.5$) for three different values of the scattering albedo: namely, $\omega = 0.0$, 0.5, and 0.9. As shown in Fig. 4, the SP-DOM results are very close to those of the LBM-FVM [19]. For $\omega = 0.0$, 0.5, and 0.9, the maximum percentage errors between the two methods are 2.9917, 3.7128, and 3.5146%, respectively.

Figure 5 shows the dimensionless temperatures Θ at different instants ζ on the centerline ($X = 0.5$) for three different values of the conduction–radiation parameter: namely, $N_{\text{cr}} = 0.01$, 0.1, and 1.0. It can be seen that for $N_{\text{cr}} = 0.01$, 0.1, and 1.0, the maximum percentage errors of SP-DOM results are 2.4917, 3.8867, and 3.5627%, respectively, as compared with those of the LBM-FVM [19].

Figure 6 shows the dimensionless temperatures Θ at different instants ζ on the centerline ($X = 0.5$) for two different values of the optical thickness: namely, $\tau_L = 0.1$ and 1.0. For both $\tau_L = 0.1$ and 1.0 cases, the maximum percentage errors between the SP-DOM and the LBM-CDM [16] are 0.7261 and 3.7654%. It is noted that the number of nodes used for the SP-DOM is $N_x \times N_y = 14 \times 14$; however, the number of control volumes/lattices used for the LBM-CDM is $N_x \times N_y = 20 \times 20$.

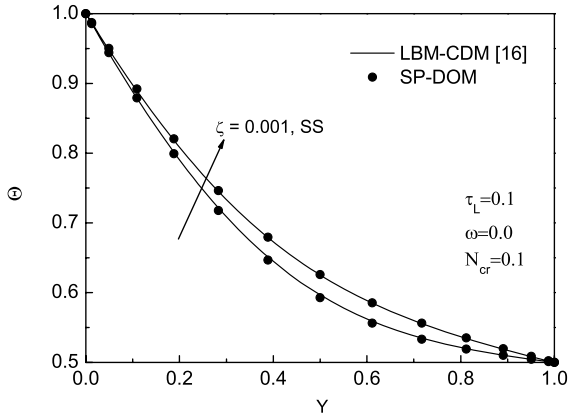

a)

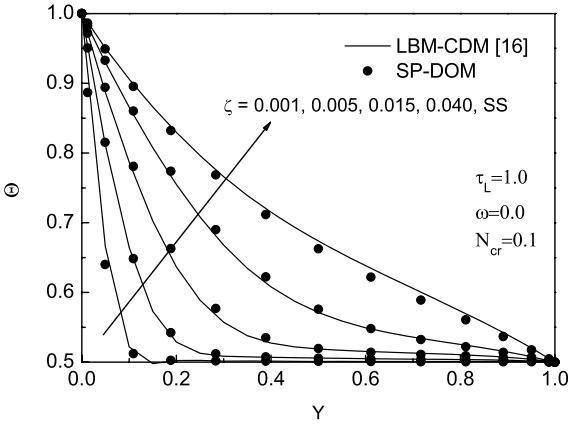

b)

Fig. 6 Dimensionless temperature Θ on centerline ($X = 0.5$) in a square enclosure at different instants ζ for optical thickness: a) $\tau_L = 0.1$, b) $\tau_L = 1.0$.

V. Conclusions

The spectral collocation method is successfully applied to solve transient coupled conduction and radiation heat transfer problems in 1-D planar and 2-D square geometries containing absorbing, emitting, and isotropically scattering media. The spatial dependence of the temperature and radiative intensity are expressed by Chebyshev polynomials, the governing equations are discretized by the spectral collocation method, and the angular dependence of radiative intensity is discretized by the DOM. Transient and steady-state medium temperature distributions are found for various values of the scattering albedo, the conduction–radiation parameter, and the optical thickness. The results of the SP-DOM are compared with available results in the literature. These comparisons indicate that the SP-DOM has good accuracy and efficiency, even using only $N = 14$ nodes and the S_8 approximation in a 1-D planar medium and using $N_x \times N_y = 14 \times 14$ and the SSD_{3b} approximation in a 2-D square enclosure.

Acknowledgment

This work was supported by the Major State Basic Research Development Program of China (no. 2006CB601203).

References

[1] Viskanta, R., and Grosh, R. J., "Heat Transfer by Simultaneous Conduction and Radiation in an Absorbing Medium," *Journal of Heat Transfer*, Vol. 84, No. 1, 1962, pp. 63–72.

[2] Viskanta, R., and Grosh, R. J., "Effect of Surface Emissivity an Heat Transfer by Simultaneous Conduction and Radiation," *International Journal of Heat and Mass Transfer*, Vol. 5, No. 8, 1962, pp. 729–734.
doi:10.1016/0017-9310(62)90203-X

[3] Razzaque, M. M., Howell, J. R., and Klein, D. E., "Coupled Radiative and Conductive Heat Transfer in a Two-Dimensional Rectangular Enclosure with Gray Medium Using Finite Elements," *Journal of Heat Transfer*, Vol. 106, No. 3, 1984, pp. 613–619.
doi:10.1115/1.3246723

[4] Sakami, M., Charette, A., and Le Dez, V., "Application of the Discrete Ordinates Method to Combined Conductive and Radiative Heat Transfer in a Two-Dimensional Complex Geometry," *Journal of Quantitative Spectroscopy and Radiative Transfer*, Vol. 56, No. 4, 1996, pp. 517–533.
doi:10.1016/0022-4073(96)00082-9

[5] Liu, L. H., and Tan, J. Y., "Meshless Local Petrov-Galerkin Approach for Coupled Radiative and Conductive Heat Transfer," *International Journal of Thermal Sciences*, Vol. 46, No. 7, 2007, pp. 672–681.
doi:10.1016/j.ijthermalsci.2006.09.005

[6] Siegel, R., and Howell, J. R., *Thermal Radiation Heat Transfer*, 4th ed., Taylor & Francis, Washington, D.C., 2002.

[7] Modest, M. F., *Radiative Heat Transfer*, 2nd ed., Academic Press, San Diego, CA, 2003.

[8] Barker, C., and Sutton, W. H., "Transient Radiation and Conduction Heat Transfer in a Gray Participating Medium with Semitransparent Boundaries," *Developments in Radiative Heat Transfer*, Vol. 49, ASME Heat Transfer Div., New York, 1985, pp. 25–36.

[9] Sutton, W. H., "A Short Time Solution for Coupled Conduction and Radiation in a Participating Slab Geometry," *Journal of Heat Transfer*, Vol. 108, No. 2, 1986, pp. 465–466. doi:10.1115/1.3246949

[10] Tsai, J. H., and Lin, J. D., "Transient Combined Conduction and Radiation with Anisotropic Scattering," *Journal of Thermophysics and Heat Transfer*, Vol. 4, No. 1, 1990, pp. 92–97. doi:10.2514/3.29171

[11] Yi, H. L., Xie, M., and Tan, H. P., "Transient Coupled Heat Transfer in an Anisotropic Scattering Composite Slab with Semitransparent Surfaces," *International Journal of Heat and Mass Transfer*, Vol. 51, Nos. 25–26, 2008, pp. 5918–5930. doi:10.1016/j.ijheatmasstransfer.2008.04.054

[12] Wu, C. Y., and Ou, N. R., "Transient Two-Dimensional Radiative and Conductive Heat Transfer in a Scattering Medium," *International Journal of Heat and Mass Transfer*, Vol. 37, No. 17, 1994, pp. 2675–2686. doi:10.1016/0017-9310(94)90384-0

[13] Liu, L. H., and Tan, H. P., "Transient Radiation and Conduction in a Two Dimensional Participating Cylinder Subjected to a Pulse Irradiation," *International Journal of Thermal Sciences*, Vol. 40, No. 10, 2001, pp. 877–889. doi:10.1016/S1290-0729(01)01274-1

[14] Talukdar, P., and Mishra, S. C., "Transient Conduction and Radiation Heat Transfer With Heat Generation in a Participating Medium Using the Collapsed Dimension Method," *Numerical Heat Transfer, Part A, Applications*, Vol. 39, No. 1, 2001, pp. 79–100. doi:10.1080/104077801458474

[15] Mishra, S. C., Talukdar, P., Trimis, D., and Durst, F., "Computational Efficiency Improvements of the Radiative Transfer Problems with or Without Conduction–A Comparison of the Collapsed Dimension Method and the Discrete Transfer Method," *International Journal of Heat and Mass Transfer*, Vol. 46, No. 16, 2003, pp. 3083–3095. doi:10.1016/S0017-9310(03)00075-9

[16] Mishra, S. C., Lankadasu, A., and Beronov, K. N., "Application of the Lattice Boltzmann Method for Solving the Energy Equation of a 2-D Transient Conduction-Radiation Problem," *International Journal of Heat and Mass Transfer*, Vol. 48, No. 17, 2005, pp. 3648–3659. doi:10.1016/j.ijheatmasstransfer.2004.10.041

[17] Mondal, B., and Mishra, S. C., "Application of the Lattice Boltzmann Method and the Discrete Ordinates Method for Solving Transient Conduction and Radiation Heat Transfer Problems," *Numerical Heat Transfer, Part A, Applications*, Vol. 52, No. 8, 2007, pp. 757–775. doi:10.1080/10407780701347663

[18] Mishra, S. C., and Roy, H. K., "Solving Transient Conduction and Radiation Heat Transfer Problems Using the Lattice Boltzmann Method and the Finite Volume Method," *Journal of Computational Physics*, Vol. 223, No. 1, 2007, pp. 89–107. doi:10.1016/j.jcp.2006.08.021

[19] Mondal, B., and Mishra, S. C., "Lattice Boltzmann Method Applied to the Solution of the Energy Equations of the Transient Conduction and Radiation Problems on Nonuniform Lattices," *International Journal of Heat and Mass Transfer*, Vol. 51, Nos. 1–2, 2008, pp. 68–82. doi:10.1016/j.ijheatmasstransfer.2007.04.030

[20] Furmanski, P., and Banaszek, J., "Finite Element Analysis of Concurrent Radiation and Conduction in Participating Media," *Journal of Quantitative Spectroscopy and Radiative Transfer*, Vol. 84, No. 4, 2004, pp. 563–573. doi:10.1016/S0022-4073(03)00273-5

[21] David, L., Nacer, B., Pascal, B., and Gerard, J., "Transient Radiative and Conductive Heat Transfer in Nongray Semitransparent Two-Dimensional Media with Mixed Boundary Conditions," *Heat and Mass Transfer*, Vol. 42, No. 4, 2006, pp. 322–337. doi:10.1007/s00231-005-0023-4

[22] Asllanaj, F., Parent, G., and Jeandel, G., "Transient Radiation and Conduction Heat Transfer in a Gray Absorbing-Emitting Medium Applied on Two-Dimensional Complex-Shaped Domains," *Numerical Heat Transfer, Part B, Fundamentals*, Vol. 52, No. 2, 2007, pp. 179–200. doi:10.1080/10407790701227351

[23] Luo, J. F., Chang, S. L., Yang, J. K., Shen, X., and Inoussa, G., "Transient Coupled Heat Transfer in a Rectangular Medium with Black Surfaces," *Journal of Quantitative Spectroscopy and Radiative Transfer*, Vol. 109, No. 15, 2008, pp. 2603–2612. doi:10.1016/j.jqsrt.2008.07.001

[24] Gottlieb, D., and Orszag, S. A., *Numerical Analysis of Spectral Methods: Theory and Applications*, Society for Industrial and Applied Mathematics, Philadelphia, 1977.

[25] Canuto, C., Hussaini, M. Y., Quarteroni, A., and Zang, T. A., *Spectral Methods in Fluid Dynamics*, Springer–Verlag, New York, 1988.

[26] Peyret, R., *Spectral Methods for Incompressible Viscous Flow*, Springer–Verlag, New York, 2002.

[27] Belgacem, F. B., and Grundmann, M., "Approximation of the Wave and Electromagnetic Diffusion Equations by Spectral Methods," *SIAM Journal on Scientific Computing*, Vol. 20, No. 1, 1998, pp. 13–32. doi:10.1137/S1064827595294344

[28] Shan, X. W., and Montgomery, D., "Magnetohydrodynamic Stabilization Through Rotation," *Physical Review Letters*, Vol. 73, No. 12, 1994, pp. 1624–1627. doi:10.1103/PhysRevLett.73.1624

[29] Chawla, T. C., and Chan, S. H., "Solution of Radiation-Conduction Problems with Collocation Method Using B-Splines as Approximating Functions," *International Journal of Heat and Mass Transfer*, Vol. 22, No. 12, 1979, pp. 1657–1667. doi:10.1016/0017-9310(79)90082-6

[30] Kamiuto, K., "Chebyshev Collocation Method for Solving the Radiative Transfer Equation," *Journal of Quantitative Spectroscopy and Radiative Transfer*, Vol. 35, No. 4, 1986, pp. 329–336. doi:10.1016/0022-4073(86)90084-1

[31] Zenouzi, M., and Yener, Y., "Simultaneous Radiation and Natural Convection in Vertical Slots," *Developments in Radiative Heat Transfer*, Vol. 203, ASME Heat Transfer Div., New York, 1992, pp. 179–186.

[32] Kuo, D. C., Morales, J. C., and Ball, K. S., "Combined Natural Convection and Volumetric Radiation in a Horizontal Annulus: Spectral and Finite Volume Predictions," *Journal of Heat Transfer*, Vol. 121, No. 3, 1999, pp. 610–615. doi:10.1115/1.2826023

[33] De Oliveira, J. V. P., Cardona, A. V., Vilhena, M. T., and Barros, R. C., "A Semi-Analytical Numerical Method for Time-Dependent Radiative Transfer Problems in Slab Geometry with Coherent Isotropic Scattering," *Journal of Quantitative Spectroscopy and Radiative Transfer*, Vol. 73, No. 1, 2002, pp. 55–62. doi:10.1016/S0022-4073(01)00169-8

[34] Lara, F. E., and Rieutord, M., "The Dynamics of a Fully Radiative Rapidly Rotating Star Enclosed Within a Spherical Box," *Astronomy and Astrophysics*, Vol. 470, No. 3, 2007, pp. 1013–1022. doi:10.1051/0004-6361:20077263

[35] Modest, M. F., and Yang, J., "Elliptic PDE Formulation and Boundary Conditions of the Spherical Harmonics Method of Arbitrary Order for General Three-Dimensional Geometries," *Journal of Quantitative Spectroscopy and Radiative Transfer*, Vol. 109, No. 9, 2008, pp. 1641–1666. doi:10.1016/j.jqsrt.2007.12.018

[36] Li, B. W., Sun, Y. S., and Yu, Y., "Iterative and Direct Chebyshev Collocation Spectral Methods for One-Dimensional Radiative Heat Transfer," *International Journal of Heat and Mass Transfer*, Vol. 51, Nos. 25–26, 2008, pp. 5887–5894. doi:10.1016/j.ijheatmasstransfer.2008.04.048

[37] Sun, Y. S., and Li, B. W., "Chebyshev Collocation Spectral Method for One-Dimensional Radiative Heat Transfer in Graded Index Media," *International Journal of Thermal Sciences*, Vol. 48, No. 4, 2009, pp. 691–698. doi:10.1016/j.ijthermalsci.2008.07.003

[38] Li, B. W., Sun, Y. S., and Zhang, D. W., "Chebyshev Collocation Spectral Methods for Coupled Radiation and Conduction in a Concentric Spherical Participating Medium," *Journal of Heat Transfer*, Vol. 131, No. 6, 2009, Paper 062701. doi:10.1115/1.3090617

[39] Sun, Y. S., and Li, B. W., "Chebyshev Collocation Spectral Approach for Combined Radiation and Conduction Heat Transfer in One-Dimensional Semitransparent Medium with Graded Index," *International Journal of Heat and Mass Transfer*, Vol. 53, Nos. 7–8, 2010, pp. 1491–1497. doi:10.1016/j.ijheatmasstransfer.2009.11.047

[40] Sun, Y. S., and Li, B. W., "Spectral Collocation Method for Transient Combined Radiation and Conduction in an Anisotropic Scattering Slab with Graded Index," *Journal of Heat Transfer*, Vol. 132, No. 5, 2010, Paper 052701. doi:10.1115/1.4000444

[41] Li, B. W., Tian, S., Sun, Y. S., and Hu, Z. M., "Schur-Decomposition for 3D Matrix Equations and Its Application in Solving Radiative Discrete Ordinates Equations Discretized by Chebyshev Collocation Spectral Method," *Journal of Computational Physics*, Vol. 229, No. 4, 2010,

pp. 1198–1212.
doi:10.1016/j.jcp.2009.10.025

[42] Boyd, J. P., *Chebyshev and Fourier Spectral Methods*, 2nd ed., Dover, New York, 2001.

[43] Li, B. W., Chen, H. G., Zhou, J. H., Cao, X. Y., and Cen, K. F., "The Spherical Surface Symmetrical Equal Dividing Angular Quadrature Scheme for Discrete Ordinates Method," *Journal of Heat Transfer*, Vol. 124, No. 3, 2002, pp. 482–490.
doi:10.1115/1.1459731

[44] Yuen, W. W., and Takara, E. E., "Analysis of Combined Conductive-Radiative Heat Transfer in a Two-Dimensional Rectangular Enclosure with a Gray Medium," *Journal of Heat Transfer*, Vol. 110, No. 2, 1988, pp. 468–474.
doi:10.1115/1.3250509

[45] Mahanta, P., and Mishra, S. C., "Collapsed Dimension Method Applied to Radiative Transfer Problems in Complex Enclosures with Participating Medium," *Numerical Heat Transfer, Part B, Fundamentals*, Vol. 42, No. 4, 2002, pp. 367–388.
doi:10.1080/10407790190053996

[46] Talukdar, P., and Mishra, S. C., "Analysis of Conduction-Radiation Problem in Absorbing, Emitting and Anisotropically Scattering Media Using the Collapsed Dimension Method," *International Journal of Heat and Mass Transfer*, Vol. 45, No. 10, 2002, pp. 2159–2168.
doi:10.1016/S0017-9310(01)00305-2